



Rapid Pleistocene desiccation and the future of Africa's Lake Victoria

Emily J. Beverly^{a,b,*}, Joseph D. White^c, Daniel J. Peppe^b, J. Tyler Faith^{d,e}, Nick Blegen^f, Christian A. Tryon^g

^a Department of Earth and Atmospheric Sciences, University of Houston, Science and Research Building 1, 3507 Cullen Blvd, Room 214, Houston, TX 77204-5008, USA

^b Terrestrial Paleoclimatology Research Group, Department of Geosciences, Baylor University, One Bear Place #97354, Waco, TX 76798-7354, USA

^c Department of Biology, Baylor University, One Bear Place #97388, Waco, TX 76798-7388, USA

^d Natural History Museum of Utah, University of Utah, 301 Wakara Way, Salt Lake City, UT 84108, USA

^e Department of Anthropology, University of Utah, 260 S. Central Campus Drive, Salt Lake City, UT 84112, USA

^f Department of Geography, University of Cambridge, Downing Place, Cambridge, UK

^g Department of Anthropology, University of Connecticut, 354 Mansfield Road, Storrs, CT 06269, USA

ARTICLE INFO

Article history:

Received 18 February 2019

Received in revised form 30 August 2019

Accepted 1 October 2019

Available online 11 November 2019

Editor: L. Robinson

Keywords:

water budget
tropical paleoclimate
East Africa
paleosol
human evolution
climate change

ABSTRACT

The effects of precipitation changes on tropical East African ecosystems and human populations is poorly understood due to the complex interplay between global and regional processes and missing data from key regions and time periods. We generate a water-budget model for Lake Victoria, the largest tropical lake in the world, the source of the White Nile, and a region that supports some of the densest human populations in Africa, that assesses the impact of changing climate on lake levels and the rate of lake level change. Model results demonstrate that significant changes in the size and volume of Lake Victoria are possible in response to changes in temperature, precipitation, and orbital forcing. This modeling indicates that Lake Victoria can transition back and forth between modern lake levels and complete desiccation in centuries to a few millennia, which is rapid enough to allow for two previously observed desiccation events between 14–18 ka, during which time the lake drained and refilled twice. Combined observations from modeling and estimates of paleoprecipitation indicate that Lake Victoria was likely desiccated between 94–36 ka. This dry interval partially overlaps the megadrought (140–70 ka) identified in Lakes Malawi and Tanganyika further south, and the cooler, drier conditions identified in the Gulf of Aden between 75–50 ka. This prolonged desiccation was probably driven by eccentricity-enhanced precession and high-latitude forcing that affected the Congo Air Boundary convergence. Using future climate projections, our model also predicts that at current rates of temperature change and previous rates of lake level fall, Lake Victoria could have no outlet to the White Nile within 10 years, and Kenya could lose access to the lake in <400 years, which would significantly affect the economic resources supplied by Lake Victoria to the East African Community.

© 2019 Elsevier B.V. All rights reserved.

1. Introduction

Terrestrial ecosystems and human populations across Africa are sensitive to changes in climate, and particularly to variability in precipitation. The recent severe drought in 2010–2011 affected more than 10 million people in Kenya, Somalia, and Ethiopia, and thus, an improved understanding of East African climate and ecological responses to future climate change is vital for the East African Community (Lyon and Vigaud, 2017). All future projections

for climate indicate that East Africa will experience increased temperatures, but despite the observed increase in drought frequency and decline of precipitation during the long rains between March and May, climate models project an increase in rainfall (Lyon and Vigaud, 2017). This disconnect between modeled and observed precipitation trends has been termed the East African climate paradox (Rowell et al., 2015). Therefore, if East Africa will become wetter in the future due to anthropogenic climate change remains an open question (Lyon and Vigaud, 2017; Niang et al., 2014). Climatic variability in tropical Africa is complex and influenced by the dynamic interplay between global and regional processes including orbital forcing, the position and intensity of what has historically been referred to as the Intertropical Convergence Zone (ITCZ), the Congo Air Boundary (CAB), high-latitude processes,

* Corresponding author at: Department of Earth and Atmospheric Sciences, University of Houston, Science and Research Building 1, 3507 Cullen Blvd, Room 214, Houston, TX 77204-5008, USA.

E-mail address: ejbeverly@uh.edu (E.J. Beverly).

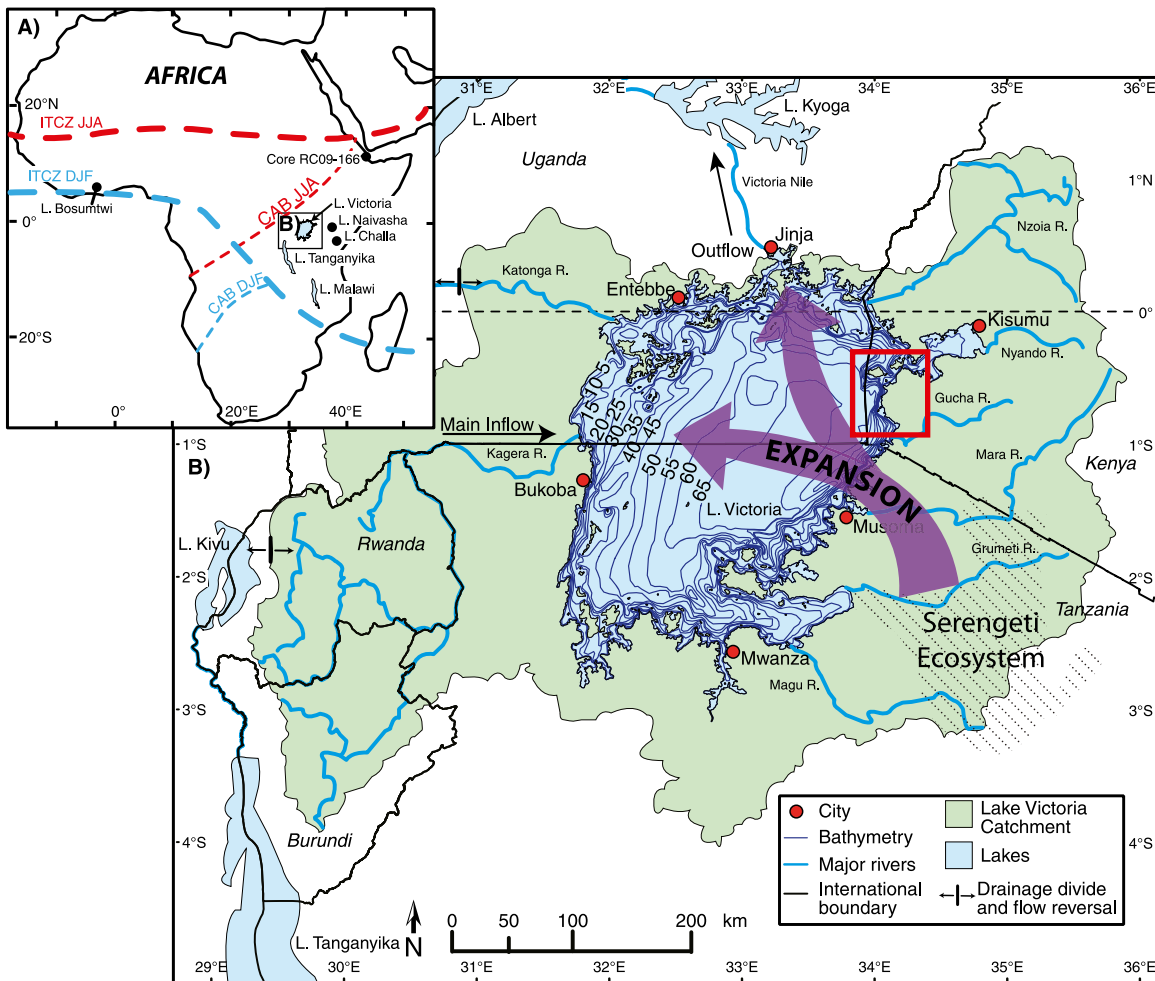


Fig. 1. Location of study. (A) Locations of lakes relevant to study including: Victoria, Naivasha, Challa, Tanganyika, Malawi, and Bosumtwi. The position of the ITCZ and CAB during June, July, and August and during December, January, and February are indicated (Nicholson, 1996). (B) The catchment of Lake Victoria with major rivers, bathymetry of the lake, and modern extent of the Serengeti Ecosystem is also indicated. In the red box, is the location of Karungu, Mfangano Island, and Rusinga Island where the paleosol samples were collected for paleosol-based proxies for precipitation. See Beverly et al. (2017, 2015) for detailed mapping of outcrops.

and tropical sea surface temperatures (SSTs) (Costa et al., 2014; Nicholson, 2018; Scholz et al., 2007; Stager et al., 2011). Fully resolving the effects of this interplay is difficult because climate station coverage across much of East Africa is poor and often interrupted, but robust paleoclimate records can address this shortcoming.

The African Great Lakes (Victoria, Malawi, and Tanganyika) are archives of climate change and together document variability in lake levels and precipitation driven by a variety of climate forcing mechanisms throughout the Quaternary (Berke et al., 2012; Costa et al., 2014; Ivory et al., 2016; Scholz et al., 2007). The Lake Victoria Basin, which straddles the equator between the eastern and western branches of the East Africa Rift System, is the largest freshwater lake in the tropics by surface area (68,800 km²) (Nicholson, 1996). The lake's location enables a study to address questions about the effects of equatorial climate change on the region, importance for subsistence and economic resources, and role in understanding the effects on human evolution and migration (Fig. 1A).

1.1. Hydrology of Lake Victoria

Lake Victoria's water budget is constrained by the low water runoff from a relatively small catchment. There is little annual temperature variability at Lake Victoria, but precipitation varies

considerably and is controlled by the seasonal rainfall migration, creating rainy seasons in March and in October (Nicholson, 2018, 1996). Precipitation is also controlled by the movement of the CAB, the strength of the Indian and Atlantic monsoons, and topography (Nicholson, 2018, 1996; Stager et al., 2011). Because of poor climate station coverage and interruptions in recording periods, reported mean annual precipitation (MAP) varies significantly across the catchment, but the most commonly reported ranges are between 1.40 and 1.80 meters per year (m yr⁻¹) (Sutcliffe and Parks, 1999; Yin and Nicholson, 1998). MAP is almost equal to average evaporation (1.46 m yr⁻¹), with local precipitation derived primarily from the lake itself, and thus, lake level responds directly to changes in rainfall (Broecker et al., 1998; Milly, 1999; Yin and Nicholson, 1998). Additionally, the lake fills a basin between the two arms of the East African rift that is wide and shallow (maximum depth 79 m) (Nicholson, 1996). This geometry results in large changes in surface area with small changes in depth relative to other African Great Lakes with large border faults forming half-grabens that result in long, narrow, and very deep lakes (700–1400 m) (Fig. 1B; Danley et al., 2012).

The effect of a shallow basin configuration is amplified because ~80% of the inflow to the lake is direct input from recycled lake water with only ~20% contributed by rivers. In addition, Lake Victoria comprises >26% of the total catchment area in comparison to Lakes Turkana (5%), Tanganyika (13%), and Malawi

(19%) (Shahin, 1985). Therefore, catchment processes including precipitation interception and runoff are less important than direct rainfall reception and evaporation of the lake itself. The Kagera River, which drains the highlands of Rwanda and Burundi, is the main inflow and accounts for >10% of the overall inflow into the lake (Fig. 1B) (Shahin, 1985; Sutcliffe and Parks, 1999; Yin and Nicholson, 1998). Because of the high proportion of inflow from the Burundi Highlands, precipitation contributions from the west from the Atlantic (via the Congo) and the east from the Indian Oceans are important to the hydrology of Lake Victoria. The lake is hydrologically open, and the only outflow is currently through the Victoria or White Nile at Jinja (Fig. 1B). Outflow is now controlled by the Nalubaale Dam, which was constructed in 1954, and outflow is managed using fluctuations in climate in an attempt to mimic natural discharge (Sutcliffe and Petersen, 2007).

Victoria's lake levels have been extremely variable since the Last Glacial Maximum (LGM), with the lake desiccating at least twice at 17 ka and 15 ka based on the identification of two paleosols in core V95-2P (Johnson et al., 1996; Stager et al., 2011; Talbot and Williams, 2009), and possibly expanding during the African Humid Period (Costa et al., 2014). Desiccations have been attributed to high-latitude forcing (Stager et al., 2011) and the migration of the CAB (Costa et al., 2014). Therefore, in addition to being an archive of equatorial climate, Lake Victoria's climate is affected by different forcing mechanisms than the other African Great Lakes, suggesting that the expression of climate may be considerably different than in tropical eastern and western Africa.

1.2. Paleoprecipitation reconstructed from paleosol-based proxies

Paleosol-based proxies have been applied to the paleosols from six sites along a ~55 km north to south transect along the eastern margin of the lake and used to reconstruct paleoprecipitation during the late Pleistocene in the Lake Victoria Basin (Beverly et al., 2017, 2015). The climate reconstructions using 1) the chemical index of alteration minus potassium (CIA-K) (Sheldon et al., 2002), 2) Paleosol Paleoclimate Model (PPM_{1.0}) (Stinchcomb et al., 2016), and 3) CALMAG (Nordt and Driese, 2010) methods indicate an average MAP of 0.75 ± 0.11 m yr⁻¹, 0.80 ± 0.18 m yr⁻¹, and 1.01 ± 0.23 m yr⁻¹, respectively (Beverly et al., 2017, 2015). Assuming a modern MAP of 1.40 m yr⁻¹, this indicates that average precipitation during parts of the late Pleistocene prior to the LGM was between 54 and 72% of modern. Data from these paleosols are used here as input variables for a new water budget model of paleo-Lake Victoria developed for this study.

2. Materials and methods

Previous water budget models (Broecker et al., 1998; Milly, 1999) indicate that Lake Victoria would be reduced to <10% of current surface area with a MAP between 0.75 and 1.01 m yr⁻¹, but these models do not assess how changes in temperature, evaporation, or insolation would influence lake level in the past, or estimate the rate of surface area loss. Here we couple previously published data from paleosol-based paleoprecipitation proxies (Beverly et al., 2017, 2015) with a new water budget model to assess the effect of climate variability on Victoria's lake levels during the late Pleistocene and to determine the expression of the megadrought in equatorial Africa. Fig. 2 shows a schematic diagram of the model and the variables are summarized in Table 1. Using models of future climate change (Sweagudde, 2009), we then use the water budget model to predict the effects of future climate change on Lake Victoria.

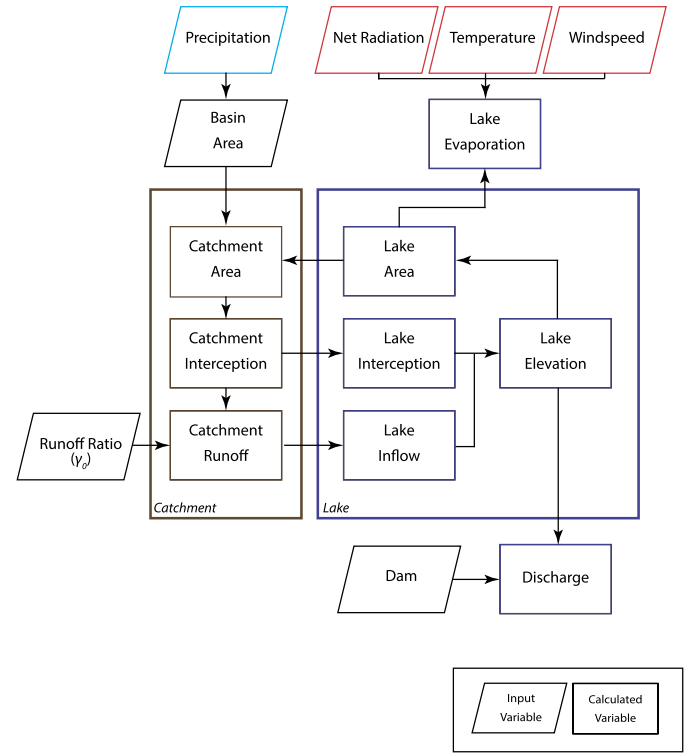


Fig. 2. A schematic diagram of the water budget model created for Lake Victoria which shows the relationship between the input and calculated variables. Shown are the relationship between the catchment and lake area that is moderated by the lake elevation dominated by the balance of precipitation and evaporation.

2.1. Adapted Penman equation for evaporation

The Penman equation was adapted for modeling the water balance of Lake Victoria:

$$\lambda E = \frac{\Delta R_n + \rho c_p (e_s - e_a) f(U_2)}{\Delta + \gamma} \quad (1)$$

where λ is latent heat of water evaporation ($\text{J g}^{-1} \text{K}^{-1}$), E is evaporative mass flux density ($\text{g m}^{-2} \text{s}^{-1}$), Δ is slope of saturated vapor pressure with temperature (Pa K^{-1}), R_n is net short and longwave radiation (W m^{-2}), ρ is density of saturated air (g m^{-3}), c_p is specific heat of air ($\text{J g}^{-1} \text{K}^{-1}$), e_s is saturated vapor pressure for the daily mean temperature (Pa), e_a is daily ambient vapor pressure (Pa), $f(U_2)$ is wind speed function utilizing ($\text{m s}^{-1} \text{Pa}^{-1}$), and γ is psychometric "constant" (Pa K^{-1}).

We estimated R_n by:

$$R_n = (1 - \alpha) SW - LW. \quad (2)$$

Shortwave radiation (SW ; W m^{-2}) is estimated as 220 W m^{-2} based on satellite observations and annual averages for Jinja, Entebbe, Kisumu, Bukoba, and Mwanza that range from 185 to 230 W m^{-2} (Shahin, 1985). Albedo (α) of shortwave radiation was estimated to be a value of 0.07 based on Lake Victoria's latitude (Cogley, 1979). For emitted longwave radiation (LW ; W m^{-2}), we estimated flux density based on the method presented by Budyko (1974):

$$LW = \varepsilon \sigma T_K^4 (0.39 - 0.058 \sqrt{e_s / 1.33322}) (1 - 0.54 C^2) \quad (3)$$

where ε is emissivity set here at a value 0.96 (Budyko, 1974), σ is Stefan Boltzmann constant ($5.67 \times 10^{-8} \text{ W m}^{-2} \text{K}^{-4}$), T_K is daily mean temperature (K), e_s^* is saturated vapor pressure in mm Hg, and C is the cloudiness in fraction of sky cover which is assumed

Table 1
Variables used in the water budget models for Lake Victoria.

Parameter	Description	Value	Units	Notes
λ	latent heat of water evaporation	–	$\text{J g}^{-1} \text{K}^{-1}$	calculated by polynomial approximation of daily mean temperature
E	evaporative mass flux density	–	$\text{g m}^{-2} \text{s}^{-1}$	calculated from the Penman-Monteith equation
Δ	slope of saturated vapor pressure with temperature	–	Pa K^{-1}	calculated from mean daily temperature and the saturated vapor pressure
R_n	net short and longwave radiation	–	W m^{-2}	calculated from short- and long-wave radiation
ρ	density of saturated air	–	g m^{-3}	calculated from the mass of dry air, the ambient vapor pressure and daily temperature
c_p	specific heat of air	1.012	$\text{J g}^{-1} \text{K}^{-1}$	Constant
e_s	saturated vapor pressure for the daily mean temperature	–	Pa	calculated from the Tetens's equation using maximum daily temperature
e_a	daily ambient vapor pressure	–	Pa	calculated from the Tetens's equation using minimum daily temperature
γ	psychometric "constant"	–	Pa K^{-1}	calculated from pressure, the latent heat of water evaporation, and the mass of air
SW	shortwave radiation	220	W m^{-2}	(Shahin, 1985)
α	Albedo	0.07	–	(Cogley, 1979)
LW	longwave radiation	–	W m^{-2}	calculated after Budyko (1974)
ε	emissivity	0.96	–	(Budyko, 1974)
σ	Stefan Boltzmann constant	5.67×10^{-8}	$\text{W m}^{-2} \text{K}^{-4}$	Constant
T_K	daily mean temperature	294.45	K	(East African Meteorological Department, 1972)
e_s^*	saturated vapor pressure	–	mm Hg	calculated from the Tetens's equation using maximum daily temperature
C	cloudiness in fraction of sky cover	0.5	–	(Yin and Nicholson, 1998; East African Meteorological Department, 1972)
M_w	molecular mass of water	18.02	g mol^{-1}	Constant
R	gas constant	8.3143	$\text{mol}^{-1} \text{K}^{-1}$	Constant
T_{Cmean}	mean maximum temperature	21.3	$^{\circ}\text{C}$	(East African Meteorological Department, 1972)
T_{Cmin}	mean minimum temperature	17.1	$^{\circ}\text{C}$	(East African Meteorological Department, 1972)
M_a	mean mass of dry air	28.96	g mol^{-1}	Constant
P	mean air pressure	–	Pa	calculated as function of mean elevation of surface of Lake Victoria
$elev$	mean elevation of surface of Lake Victoria	1135	m	(Shahin, 1985)
A_L	lake area	–	m^2	calculated as a function of lake level height
U_2	average wind speed measured at a 2 m reference height	2.2	m s^{-1}	(McJannet et al., 2012)
Δh	change in annual height of the water	–	m yr^{-1}	calculated
P_C	annual catchment precipitation interception	–	m	(Howell et al., 1988; Sutcliffe and Parks, 1999)
γ_0	catchment precipitation runoff ratio for time = 0	0.08	–	(Shahin, 1985)
P_L	annual lake precipitation interception	–	m	(Howell et al., 1988; Sutcliffe and Parks, 1999)
E_L	lake precipitation	–	m yr^{-1}	(Howell et al., 1988; Sutcliffe and Parks, 1999)
R_L	discharge from the lake	–	m	(Howell et al., 1988; Sutcliffe and Parks, 1999)
ρ_w	density of liquid water	–	g cm^{-3}	calculated as a function of temperature
Q	Nile River discharge at Jinja	–	$\text{m}^3 \text{s}^{-1}$	(Howell et al., 1988; Sutcliffe and Parks, 1999)
P_p	mean annual precipitation in the past	0.75 to 1.01	m yr^{-1}	(Beverly et al., 2015, 2017)
R_1	value of the past catchment runoff	–	m yr^{-1}	(Wigley and Jones, 1985)
α	fraction of precipitation in the past relative to the current	0.54 to 0.72	–	(Beverly et al., 2015, 2017)
β	function that represents the change in catchment evapotranspiration under a different climate than the present	–	–	(Wigley and Jones, 1985)
a	fraction of catchment area covered by vegetation	0.25	–	(Claussen et al., 1999)

to be 0.50 based on previous water budget studies of Lake Victoria (Yin and Nicholson, 1998) and averages from shoreline meteorological stations (East African Meteorological Department, 1972).

The value of Δ for equation (3) was calculated by:

$$\Delta = \frac{\lambda M_w e_s}{RT_K} \quad (4)$$

where M_w is the molecular mass of water (18.02 g mol^{-1}) and R is the gas constant ($8.3143 \text{ J mol}^{-1} \text{K}^{-1}$). The value of λ was derived by polynomial approximation as a function of daily mean temperature (T_C , $^{\circ}\text{C}$):

$$\lambda = 2500.8 - 2.36T_C + 0.0016T_C^2 - 0.00006T_C^3 \quad (5)$$

The values of e_s and e_a (e_i) were approximated from the Tetens formula:

$$e_i = 611e^{\left(\frac{17.502T_C}{240.97+T_C}\right)} \quad (6)$$

where T_C is mean temperature ($^{\circ}\text{C}$). The mean maximum temperature from 6 stations (Entebbe, Jinja, Kisumu, Musoma, Mwanza,

and Bukoba) (21.3°C) was used to calculate e_s . For e_a a mean minimum temperature of 17.1°C (East African Meteorological Department, 1972) was used as a surrogate estimate of dew point temperature appropriate for non-arid climates (Glassy and Running, 1994). The air directly Lake Victoria is near saturation with density of air (ρ) calculated as moist air as a function of temperature:

$$\rho = \{M_w e_a + M_a (P - e_a)\} / RT_K \quad (7)$$

where M_a is mean mass of dry air (28.96 g mol^{-1}) and P is the mean air pressure (Pa) with the air pressure was approximated by:

$$P = 101300 e^{(-elev/8200)} \quad (8)$$

where $elev$ is mean elevation of the surface of Lake Victoria set here at 1135 m after construction of the Nalubaale Dam. For the model, P is considered dynamically with changes in lake storage and resultant elevation.

The value of γ in equation (3) varied slightly with temperature due to the influence on λ . The value was estimated by:

$$\gamma = \frac{c_p P}{\lambda(M_w/M_a)} \quad (9)$$

where a constant value of $1.012 \text{ J g}^{-1} \text{ K}^{-1}$ was assumed for c_p .

The use of the wind function (i.e. $f(U_2)$) as a modifier of vapor pressure difference in equation (3) 1) avoids the need for specific resistance, 2) is consistent with the original formulation of the Penman equation, and 3) allows for inclusion of lake morphology as a variable affecting open water evaporation. McJannet et al. (2012) proposed a wind function for open water that included lake area (A_L) as a variable where:

$$f(U_2) = (2.36 + 1.67U_2)A_L^{-0.05} \quad (10)$$

with an average wind speed of 2.2 m s^{-1} measured at a 2 m reference height (U_2) with output units of the $f(U_2)$ in $\text{mm d}^{-1} \text{ kPa}^{-1}$. For unit consistency in our adapted Penman equation, the units of the original McJannet et al. (2012) formula were converted into units of $\text{m s}^{-1} \text{ Pa}^{-1}$. The value of using this function rather than a bulk resistance (sensu, Monteith and Unsworth, 2008) is that the change in area of the lake over time is included a feedback to evaporation in the water balance calculation.

2.2. Modeling the present lake level

Researchers have studied the water balance of Lake Victoria since the 1930s with models resulting in imbalanced inflows and outflows (Broecker et al., 1998). Yin and Nicholson (1998) summarized past modeling efforts and identified that the main problem with simulated water balance of the lake are from calculated variables including: precipitation and evaporation and to a lesser degree the lack of stream inflow measurements. Precipitation estimates for Lake Victoria are variable due to inconsistent station coverage that are concentrated in Kenya and Tanzania and interruptions in recording periods (Yin and Nicholson, 1998). As a result, early models often balanced the water budget by increasing or decreasing precipitation and later models modified evaporation (Yin and Nicholson, 1998, and references therein). More recent and advanced modeling calculates lake level fluctuation on a daily basis (Vanderkelen et al., 2018); however, the purpose of this model is to understand paleo-lake levels, and therefore, a simpler model is more appropriate, similar to the model by Lyons et al. (2011) for the Lake Malawi Basin.

The models developed here are available in Supplementary Datasets S1-S4. The lake water was modeled based on a simple water balance approach:

$$\Delta h = P_C \gamma_0 + P_L - E_L - R_L \quad (11)$$

where Δh is change in annual height of the water (m yr^{-1}), P_C is annual catchment precipitation (m), γ_0 is catchment precipitation runoff ratio (dimensionless) for time = 0, P_L is annual lake precipitation (m), E_L is lake precipitation ($[E_L = (E/\lambda)(1/\rho_w)(365 \cdot 86400)]$) in m yr^{-1} , and R_L is discharge from the lake (m) assuming that the lake is the outlet structure of the catchment where 365 is the number of days per year and 86,400 is the number of seconds per day. Groundwater inflow or outflow is assumed to be negligible because in relation to other water balance fluxes (precipitation and evaporation) groundwater interaction is insignificant (Sweagudde, 2009).

To evaluate this model, two sets of observed precipitation and lake discharge data from 1956 to 1978 (Howell et al., 1988; Sutcliffe and Parks, 1999) were used. The model accuracy was only tested using data from 1965 to 1978 to avoid changes in lake level due to dam construction in 1954 (Sutcliffe and Parks, 1999). We assumed P_C was equal to P_L , and for R_L , observed values for the Jinja station were derived from the “agreed-upon curve”

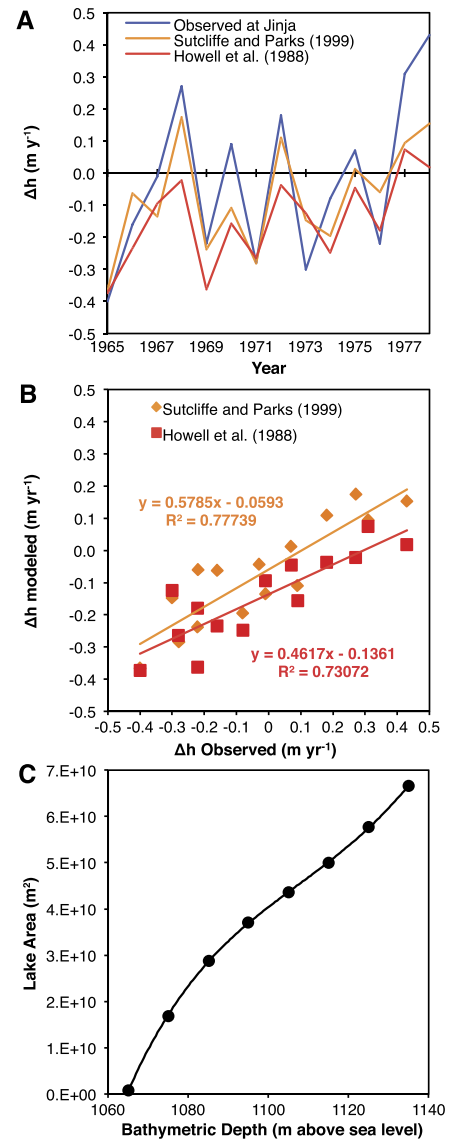


Fig. 3. Results of the modern water budget modeling comparing observed vs. model-predicted values for change in lake level height to evaluate the accuracy of the model and the analyses used to relate lake area to bathymetry. (A) Comparison of the change in annual height of the lake (Δh) with modeled results from two different datasets: Sutcliffe and Parks (1999) and Howell et al. (1988), and the observed values measured at Jinja (Sutcliffe and Petersen, 2007) for the years 1965 to 1978. (B) Observed Δh vs. modeled Δh with simple linear regression resulting in a slightly better R^2 value of 0.78 for the Sutcliffe and Parks (1999) dataset that is therefore used in development of the model. (C) Bathymetric analysis of Lake Victoria that relates depth in m above sea level to lake area using a fourth-order polynomial function (Eq. (12)), which is used to calculate changes in lake area in Fig. 4D.

(Sutcliffe and Petersen, 2007). For γ_0 , a value of 0.08 was used for the Lake Victoria catchment (Shahin, 1985), a value similar to 0.10 estimated for the entire Nile River (Wigley and Jones, 1985). With these input data, Δh was calculated and compared with observed values (Fig. 3A). Least square regression analysis showed moderately high correlation ($r^2 = 0.78$) between modeled and Δh using Sutcliffe and Parks (1999) input indicating that lake elevation is driven by a fairly straightforward budget, constrained by P_L and E_L , similar to other studies (Figs. 3A and B; Dataset S1; Broecker et al., 1998; Milly, 1999; Sutcliffe and Petersen, 2007; Yin and Nicholson, 1998). This is also consistent with more recent models by Vanderkelen et al. (2018) where precipitation and evaporation account for approximately 77% of the lake water balance.

2.3. Bathymetric analysis of Lake Victoria

Because the depth to area/volume relationship is unique for each lake, we first georeferenced and digitized a bathymetric map for Lake Victoria (Verschuren et al., 2002). The contours were mapped at 5 m intervals, and these digitized data were captured in the form of a shapefile. All analyses were conducted in ArcGIS® (version 10.0; ESRI, Redlands, CA). To calculate area and volume values by depth, the shapefile was analyzed using the Polygon Volume function based on analysis of the individual bathymetric contours below the reference height of 1135 m. Using these data, we fit a fourth-order polynomial function using bathymetric depth as the independent variable (h) and lake area (A_L) as the dependent variable:

$$\begin{aligned} A_L = & -8.42499988041810 \times 10^2 h^4 \\ & + 3.931696313072550 \times 10^6 h^3 \\ & - 6.862506670194270 \times 10^9 h^2 \\ & + 5.311594269525770 \times 10^{12} h \\ & - 1.538663756789369 \times 10^{15} \end{aligned} \quad (12)$$

This equation is used to predict discharge in the past (Fig. 3C; Dataset S1). Changes in depth (Δh) were then used to calculate annual depth values that when applied to the derived depth to area relationship can be used to estimate A_L . This new annual value of A_L was then used as input for $f(U_2)$ affecting subsequent derived values of λE .

2.4. Changes in Lake Victoria's geometry

Uplift and tilting during the Middle Pleistocene shifted the center of the Lake Victoria basin ~ 50 km to the east (Doornkamp and Temple, 1966). There is no evidence for tectonic modification of Lake Victoria since then, suggesting that the modern lake had formed by this time, and that modern lake geometry is a reasonable input variable. However, uplift in the Toro-Ankole volcanic province (≤ 50 ka) in Uganda likely modified the drainage of Lake Victoria (Boven et al., 1998). Before uplift, outflow for Lake Victoria was likely through the Katonga and Kagera Rivers towards Lakes Albert and Edwards. This uplift caused a flow reversal of these tributaries, likely between 35 and 25 ka, and ultimately led to the formation of the modern outflow to the north through the Victoria Nile (Talbot and Williams, 2009). It is uncertain when this modern connection occurred, but probably in the last 13 ka (Talbot and Williams, 2009). The effect of any outlet on the water budget of Lake Victoria would be to increase the rate of desiccation, and thus, the Jinja outlet is used to demonstrate this effect for our model.

2.5. Calculating past lake discharge

As part of the water budget, discharge from the lake is required. Values of R_L for the analysis of lake levels for 1965 to 1978 were derived from empirical observations, though inferred from the derived values of the “agreed-upon curve” (Sutcliffe and Petersen, 2007). This curve is assumed to reflect natural discharge prior to construction of the Nalubaale Dam:

$$Q = 132.923(\Delta h - 8.486)^{1.686} \quad (13)$$

where Q is the Nile River discharge at Jinja in $\text{m}^3 \text{s}^{-1}$. To convert Q values to annual depth values for the water budget analysis,

$$R_L = (Q/A_L)(365)(86400) \quad (14)$$

where 365 is the number of days per year and 86,400 is the number of seconds per day.

At some point the value of Δh would result in complete cessation of flow into the Victoria Nile using the present morphologic characteristics of Jinja outlet. Linearization of the “agreed-upon curve” function followed by solving for Δh where $Q = 0.0$ yields a value of 1130.5 m for the cessation of Nile flow. For the model of the past, lake height value (h , where $h = 1122 \cdot \Delta h$ assuming 1122 m is the Jinja elevation as a reference point), and $R_L = 0.0$ where calculated values of $h \leq 1130.5$ m.

2.6. Modeling past lake levels

The paleoprecipitation reconstruction from the Lake Victoria paleosols by Beverly et al. (2017, 2015) indicates minimal change in average values through time, and therefore, the averaged minimum reconstructed value of 0.75 m yr^{-1} (CALMAG proxy) and maximum value of 1.01 m yr^{-1} (PPM_{1.0} proxy) are used as the input variables for the late Pleistocene water budget calculations. This provided a minimum precipitation and maximum estimate to apply to the water budget of Lake Victoria and subsequent changes of MAP in the past (P_p) which ranged from 54 and 72% of modern MAP (Sutcliffe and Parks, 1999). Next, using the methods proposed by Wigley and Jones (1985), the value of the past catchment runoff (R_1) was approximated by the equation:

$$\frac{R_1 - R_0}{R_0} = \frac{\alpha - (1 - \gamma_0)\beta}{\gamma_0} \quad (15)$$

that can be simplified to:

$$R_1 = R_0 \left(\frac{\alpha - (1 - \gamma_0)\beta}{\gamma_0} - 1 \right) \quad (16)$$

where α is the fraction of past precipitation relative to the current (0.54 to 0.72) and β is a function that represents the change in catchment evapotranspiration under a different climate than the present. For simplification, the β function was estimated as:

$$\beta \cong 1 - 0.3a \quad (17)$$

where a is the fraction of catchment area covered by vegetation. In this case, we assumed under drier conditions of the past, that only 25% of available catchment land area had vegetation cover similar to the large scale drying of the sub-Saharan savanna (Clausen et al., 1999). This is likely an overestimation, but to test this sensitivity, the model was adjusted by adding changes in vegetation in increments of 10% and evaluating the resulting impact on the model. The results of this analysis were almost indistinguishable from a model with 25% vegetation and negligible in comparison to the effects of changing precipitation or evaporation.

Changes in incident radiation were modeled to account for changes in insolation and therefore evaporation throughout the Pleistocene. Precession has the greatest influence over climate in tropical Africa and has created fluctuations in insolation over periods of 19 to 23 ka, which have a great effect on the strength of the East African monsoon (Clement et al., 2004; Scholz et al., 2007). Changes in insolation translated into simulations in which input values of SW , as part of the calculation of E_L , were varied from present mean values of 220 W m^{-2} by $\pm 37.5 \text{ W m}^{-2}$ to form the boundaries of precession maxima and minima in the last 100 ka and $+17.5 \text{ W m}^{-2}$ for the LGM. The effects of temperature changes ($\pm 2^\circ \text{C}$) were also simulated based on reconstructions from the Burundi highlands over the past 40 ka, which is the closest available paleotemperature data extending beyond the LGM (Bonneville and Chalé, 2000). Using these values to calculate lake evaporation, coupled with annual updated values of A_L and resultant R_L , annual

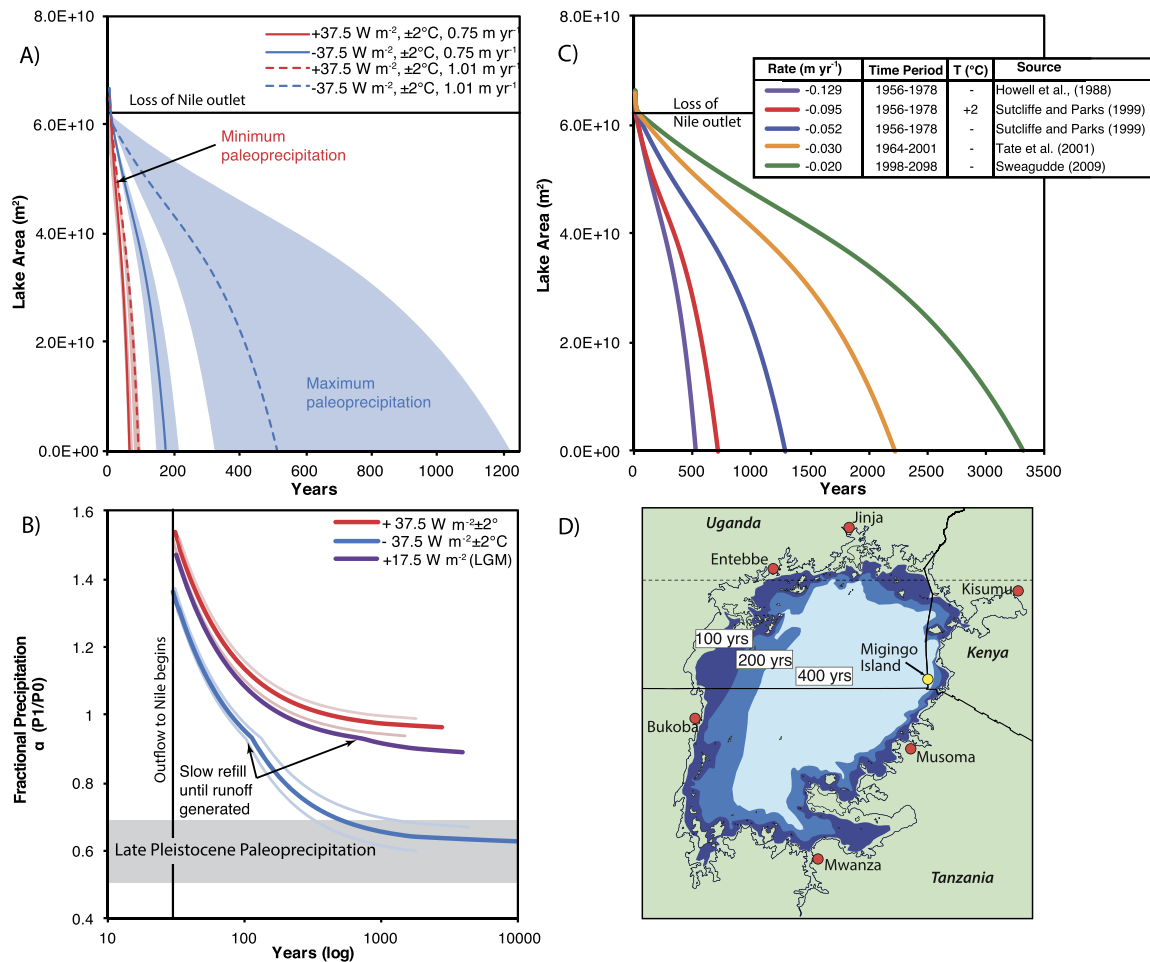


Fig. 4. Results of the water budget modeling. (A) Rates of drying of Lake Victoria based on late Pleistocene precipitation (54% of modern - solid line; 72% of modern dashed line). Maximum insolation is in red and minimum in blue with the area around the line representing the variation in temperature. Regardless of changes in temperature and insolation the lake will dry up within centuries at these precipitation values. (B) Rates of filling of Lake Victoria, which illustrates how many years it will take to fill the lake with different amounts of fractional precipitation (i.e., Pleistocene precipitation/modern precipitation). At lower temperatures and insolation values the lake can refill, but very slowly, and at higher temperatures and insolation values Lake Victoria cannot refill until runoff is generated. (C) Rates of drying a modern Lake Victoria based on model developed for this study and previous studies (e.g., Howell et al., 1988; Sutcliffe and Parks, 1999; Sweagudde, 2009), which indicates that the Victoria Nile outlet at Jinja could disappear as quickly as 10 years. Recent rates of decline projected out into the future indicate that Lake Victoria could dry up in as little as 500 to 3300 years. (D) Map of the areal extent of Lake Victoria at 100, 200, and 400 years based the Howell et al. (1988) rate in Fig. 4C (in purple), which indicates that all the major cities around Lake Victoria could lose access to the lake in as little as 100 years, and Kenya could lose all access to the lake in 400 years.

values of Δh were calculated, starting with an assumed lake elevation 1135 m (full lake), to determine the trend in elevation and potential long-term effects on the lake. The annual values of Δh were subtracted from a starting lake elevation of 1135 m to determine time to desiccation of the lake (Fig. 4A and Dataset S2).

According to our model, Lake Victoria will not refill without a threshold precipitation amount of an additional 1% above normal for the LGM scenarios to achieve outflow through Jinja. Then, the total depth of the lake (1130.5 m – 1065 m) was divided by Δh to calculate the effective time to fill Lake Victoria (Fig. 4B and Dataset S3).

2.7. Modeling future lake levels

Limited observational data indicates East African precipitation has decreased over the last 50 years, but the projected precipitation for the next 100 years is complex due to contrasting predictions between Global Climate Models (GCMs) and regional models (Lyon and Vigaud, 2017; Niang et al., 2014). Predictions of precipitation range from no change to a 20% increase in precipitation in GCMs, to a decrease in regional models (Niang et al., 2014). The Δh values calculated from the two modern datasets

(Howell et al., 1988; Sutcliffe and Parks, 1999) from 1965 to 1978 are used to determine the time to loss of the Nile outlet and desiccation of the lake from a starting elevation of 1135 m (Fig. 4C, purple and blue). Using the Sutcliffe and Parks (1999) dataset, the effect of +2°C on evaporation was also modeled to simulate a minimum estimate of climate change effects (Fig. 4C, red; Dataset S4).

3. Results

Previous research has shown that reconstructed MAP from paleosol-based proxies was between 54 to 72% of modern between 94 and 36 ka (Beverly et al., 2017). Using those values as inputs, our model generated here indicates that Lake Victoria would desiccate within a few centuries at precession maxima (+37.5 W m⁻² relative to today) regardless of temperature, and within millennia at precession minima (-37.5 W m⁻²) (Figs. 4A and 5B). This indicates that regardless of orbital parameters, Lake Victoria will rapidly desiccate (on scales of ~10² yr) when MAP is ≤75% of modern.

Once Victoria desiccated, refilling the lake to current lake level, where there is outflow via the White Nile, is either slow or requires MAP levels near modern. Under precession maxima condi-

tions, Lake Victoria cannot refill to modern levels until there is enough precipitation to generate runoff, which occurs at $\sim 96\%$ of modern MAP in our model. Once MAP reaches $>97\%$ of modern, the lake can refill rapidly within centuries. At precession minima (-37.5 W m^{-2}), Lake Victoria can be refilled with lower precipitation ($>62\%$), but refill is very slow at simulated insolation levels equivalent to precession minima ($>10 \text{ kyr}$), until enough rainfall generates runoff ($\sim 94\%$ of modern) at which point the lake refills within centuries. Using the orbital parameters that existed during the LGM ($+17.5 \text{ W m}^{-2}$), Lake Victoria could refill very slowly once MAP was $>89\%$ of modern precipitation. Once runoff is generated at 94% of modern MAP, the lake could fill within centuries.

4. Discussion

In this study, our model indicates that the desiccation and refilling of Lake Victoria can happen over relatively short time scales (i.e., centuries to millennia) and is directly tied to MAP levels and associated runoff. MAP fluctuations of this scale likely necessitate a regional forcing mechanism.

4.1. Drivers of climate variability in tropical East Africa

There are no long cores currently available from Lake Victoria, so much of what is known about the history of the lake ends at the LGM. However, a combination of seismic data and short cores have identified paleosols in the deepest portion of the lake, indicating that Lake Victoria has desiccated at least twice at 17 ka and 15 ka (Fig. 5C; Johnson et al., 1996; Stager et al., 2011; Talbot and Williams, 2009). Such rapid desiccation and refilling of the lake is consistent with our water budget model, which indicates that such changes could occur within centuries to millennia (Figs. 4A and B).

Paleosol-based proxies indicate that precipitation was between 54 and 72% of modern between 94 and 36 ka (Beverly et al., 2017, 2015), and when used as an input in our water budget model, suggest that Lake Victoria remained desiccated for that entire period. At those precipitation levels, a lake cannot be sustained at all at precession maxima (red lines; Fig. 4B) and at precession minima a lake could be supported but refill would be very slow ($\sim 10 \text{ kyr}$; blue lines Fig. 4B). A late Pleistocene desiccation surface interpolated based on sediment accumulation rates to be $\sim 80 \text{ ka}$ has been identified in seismic profiles (Stager and Johnson, 2008). This unconformity is compatible with our interpretation that Lake Victoria was likely desiccated, or nearly so, from 94 to 36 ka (Fig. 5C).

The geographic extent of these paleoprecipitation reconstructions ($\sim 1000 \text{ km}^2$) indicates that this decrease in precipitation must have been a regional phenomenon, suggesting a regional forcing mechanism. This period (94–36 ka) coincides with cooler and drier conditions in the Gulf of Aden between ~ 75 and 50 ka (Tierney et al., 2017), a generally low to desiccated Lake Naivasha between ~ 100 and 30 ka (Fig. 5D; Trauth et al., 2003), and partially overlaps with the megadrought identified in Lakes Malawi, Tanganyika, and Bosumtwi between 135 and 70 ka (Fig. 5G, Ivory et al., 2016; Johnson et al., 2016; Scholz et al., 2007). Lake levels in Malawi, Tanganyika, and Bosumtwi were all low from 135–70 ka, which then refilled and remained relatively deep (Ivory et al., 2016; Johnson et al., 2016; Scholz et al., 2007). In addition, an energy-balance hydrologic model of Lake Malawi indicates a similar decrease in precipitation (61% relative to modern) is needed to achieve the lowstand identified during the megadrought (Lyons et al., 2011).

Shifts in the ITCZ are often invoked to explain precipitation changes in tropical Africa (Scholz et al., 2007); however, based on the equatorial position of Lake Victoria, it is unlikely that the ITCZ

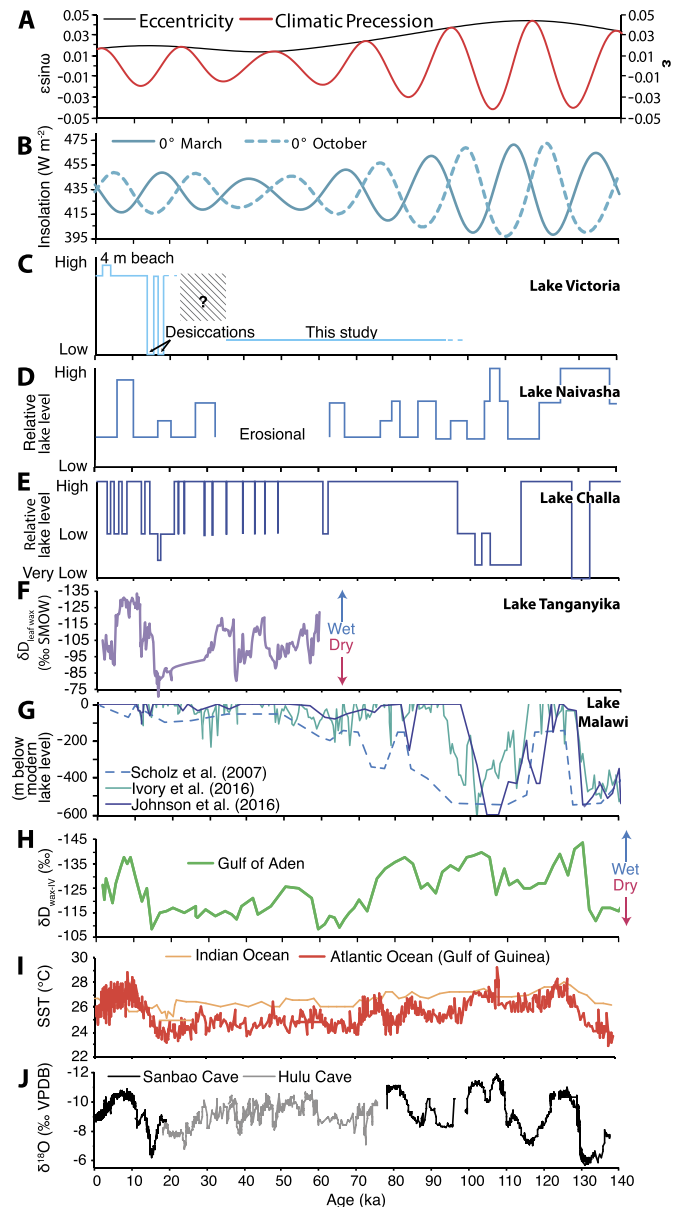


Fig. 5. (A) Eccentricity and climatic precession from 140 ka to present, which is one of major controls on tropical African climate in the past (Laskar et al., 2004). (B) Mean monthly insolation at the equator for March and October, which is used as the minimum and maximum insolation values in the water budget modeling (Laskar et al., 2004). (C) Reconstructed relative level of Lake Victoria (Johnson et al., 1996; Stager et al., 2011; this study). (D–H) These records for relative lake level and wetter and drier conditions are plotted for comparison with the Lake Victoria (this study) and show that aridity during this time period (94–36 ka) was not identical. (D) Relative level of Lake Naivasha (Trauth et al., 2003). (E) Relative level of Lake Challa (Moernaut et al., 2010). (F) $\delta D_{\text{leaf wax}}$ from Lake Tanganyika showing the relative changes from wet to dry during the past 60 ka (Tierney et al., 2008). (G) Level of Lake Malawi in meters below modern (Ivory et al., 2016; Scholz et al., 2007). (H–J) Records from the Gulf of Aden and the Atlantic and Indian Oceans, which record effects of eccentricity-enhanced precession on climate. (H) $\delta D_{\text{max iv}}$ from marine Core RC09-166 from the Gulf of Aden (Tierney et al., 2017). (I) Sea surface temperature records for the Indian and Atlantic monsoons. SSTs calibrated from the U_{37}^K record for the MD85668 core in the Indian Ocean off the coast of Somalia (Bard et al., 1997) and Mg/Ca SSTs estimates from the Gulf of Guinea in the Atlantic Ocean (Weldeab et al., 2007). (J) $\delta^{18}\text{O}$ record of the Asian monsoon from the Sanbao and Hulu Caves from China (Wang et al., 2008). The Hulu record is plotted 1.6‰ more negative to account for the higher values in the Hulu Cave (Wang et al., 2008).

could be shifted far enough to prevent its twice annual crossing over Lake Victoria. Thus, the position of the ITCZ cannot account for the late Pleistocene desiccation of Lake Victoria. Climate mod-

eling indicates that when eccentricity is high, precessional forcing is greater at low latitudes compared to high latitudes (Verschuren et al., 2009). Thus, widespread climatic variability across Africa likely peaked between 145 and 60 ka due to eccentricity-enhanced precession (Fig. 5A; Laskar et al., 2004). Climate variability in late Pleistocene low latitude records of SSTs from tropical marine records in the Atlantic (Weldeab et al., 2007) and Indian Oceans (Bard et al., 1997), and the monsoon record from East Asia (Wang et al., 2008) are all also attributed to eccentricity-enhanced precession (Figs. 5H and I). This orbital mechanism has been invoked to explain the aridity for Lakes Malawi, Tanganyika, and Bosumtwi during the 135 – 70 ka megadrought (Scholz et al., 2007), and plausibly explains the desiccation of Lake Challa from 114 – 97 ka (Moernaut et al., 2010). Thus, we posit that eccentricity-enhanced precession is the likely driver of aridity in the Lake Victoria region ~100 – 70 ka. After 70 ka, Lakes Malawi, Tanganyika, Bosumtwi and Challa begin to refill (Figs. 5E, F, and G). The refilling of these lakes is attributed to stable precipitation conditions as eccentricity decreased (Scholz et al., 2007). However, based on MAP estimates (Beverly et al., 2017) and our model projections, Lake Victoria remained desiccated until 36 ka. We propose that the shift to high-latitude forcing that began at ~70 ka affected Lake Victoria differently.

The record of desiccation from 94 to 36 ka at Lake Victoria is very similar to Lake Naivasha (Trauth et al., 2003), located ~250 km to the east of Lake Victoria at approximately the same latitude. Lake Naivasha had low-to-intermediate lake levels between 105 and 60 ka and was dry between 60 and ~35 ka based on an erosional unconformity (Figs. 1A and 5D). Because of changes in orbital forcing, the cause for extended aridity from ~70 to 36 ka in both Lakes Victoria and Naivasha must be due to factors other than eccentricity-enhanced precession (Trauth et al., 2003). Low lake levels in Lake Naivasha have been attributed to low SSTs in the Indian Ocean that weakened the East African monsoon (Bard et al., 1997; Trauth et al., 2003), but this would likely affect Lake Challa, which had high lake levels from 97 ka to the LGM. Therefore, another driver for the aridity in Lakes Victoria and Naivasha from ~70–36 ka is needed.

$\delta D_{leaf\ wax}$ records from the last 25 kyr indicate that the east-west moisture gradient across tropical Africa is related to strength of the CAB (Costa et al., 2014; Moernaut et al., 2010; Tierney et al., 2008). The strength of the CAB is influenced by SSTs in the SE Atlantic and the Indian Ocean (Bard et al., 1997; Costa et al., 2014; Weldeab et al., 2007) and changes in the tropical-subtropical SST gradient in the SE Atlantic are linked to high latitude forcing (Figs. 5I and J, Weldeab et al., 2007). Lakes Malawi and Challa are both on the Indian Ocean side of the CAB, and therefore, unaffected by changes in the Atlantic moisture supply (Fig. 1A). The CAB converges over the Lake Victoria basin, which means the lake catchment receives precipitation from both the Atlantic and Indian Oceans. Cooler SSTs in both the Indian (Bard et al., 1997) and Atlantic Oceans (Weldeab et al., 2007) are a proposed mechanism for aridity in the Lake Victoria region at 17 and 15 ka due to reduction of moisture transport and likely a weaker CAB convergence. We suggest that the extended period of aridity at Lake Victoria between 94 and 36 ka was caused by eccentricity-enhanced precession between 94 and ~70 ka (i.e., the East African megadrought), followed by high-latitude forcing causing low SSTs affecting CAB convergence from ~70 and 36 ka. Together, these forcing mechanisms maintained conditions in which precipitation was below the threshold necessary to sustain Lake Victoria. Lake Naivasha is close to the CAB, but ~250 km closer to the Indian Ocean than Lake Victoria, suggesting that the moisture from the Indian Ocean is a more important moisture source than the Atlantic and potentially explaining the intermediate aridity of Lake Naivasha from 105 to 60 ka (Fig. 5D).

4.2. Implications for early modern humans, cichlids, and other fauna

These external climate forcing mechanisms and rapid lake level fluctuations likely had a large impact on the regional biota. The Africa Great Lakes are home to ~2,000 species of cichlid fish with ~700 species in Lake Victoria alone, 150 of which are endemic (e.g., Danley et al., 2012). This rapid diversification occurred in the last 10 Myr, and climatically driven wet-dry transitions have been tied to rapid diversification events in Lake Malawi over the last 1.2 Myr (Ivory et al., 2016) and suggested to be species pumps that increased diversity in Lake Tanganyika. Desiccation surfaces in Lake Victoria are identified in the late Pleistocene at ~80 ka, 17 ka, and 15 ka (Stager et al., 2011; Stager and Johnson, 2008). Our model, together with lithologic and seismic evidence, indicates that rapid desiccation and refilling of Lake Victoria is possible in centuries to millennia and that at precession maxima rainfall <96% of modern could not sustain a lake. This suggests severe and rapid wet-dry cycles were common over the last 100 kyr at Lake Victoria and likely also influenced the evolution of Lake Victoria cichlids and led to diversification similar to Lakes Malawi and Tanganyika.

Repeated and rapid desiccation of Lake Victoria would have also affected the dispersal patterns of early modern humans and other fauna. Desiccation of Lake Victoria, would have removed a significant geographic barrier and enhanced dispersal potential as grasslands would have expanded simultaneously with the retreat of the lake (Fig. 1B; Tryon et al., 2016). Removal or reduction of Lake Victoria as a biogeographic barrier to fauna would have enhanced the Nilotic corridor as an avenue for the dispersal of early modern humans within and out of Africa (Beverly et al., 2017; Tryon et al., 2016).

4.3. The future of Lake Victoria

These results indicate rapid lake level fluctuations were common in the Lake Victoria region throughout the Pleistocene affecting the evolution of both flora and fauna. Understanding the future effects of anthropogenic climate change on Lake Victoria, is crucial for the 40 million people living in the Lake Victoria Basin and depending on the resources it provides. East Africa is projected to experience an increase in temperature between 1 and 5 °C over the next 100 years (Niang et al., 2014). Our model indicates that Lake Victoria is most sensitive to the balance of precipitation inputs and evaporation losses (Figs. 4A and B), but increased temperature will affect evaporation regardless of the direction or magnitude of precipitation change, for which climate models disagree (Lyon and Vigaud, 2017; Niang et al., 2014). Regional climate modeling also indicates that Lake Victoria cools the broader region by ~1 °C (Thiery et al., 2015). Therefore, a loss or significant reduction of the lake would only enhance projected temperature changes, which in turn would increase evaporation non-linearly (Rial et al., 2004).

Because future precipitation is uncertain with some models indicating an increase in precipitation, decrease in precipitation, or decrease in precipitation compensated by an increase in lake inflow (Lyon and Vigaud, 2017; Niang et al., 2014; Vanderkelen et al., 2018), rates of known lake level fall from several time periods are used to show how Lake Victoria has historically responded to changes in precipitation, and then projected into the future. The rate of lake level decline from the Sutcliffe and Parks (1999) data used to develop this model is on average -0.052 m yr^{-1} between 1956 and 1978 (Fig. 4C, blue). The effect of an increase in temperature of 2 °C on evaporation was also modeled to simulate the effects of climate change over the next 100 years (red line, Fig. 4C). When a +2 °C increase in temperature is modeled with the Sutcliffe and Parks (1999) dataset the rate of lake level drop

accelerates from -0.052 to -0.095 myr^{-1} (Fig. 4C, red). The average rate of decline for the huge drop in lake level between 1964 and 2002 is -0.030 myr^{-1} , which by extension could dry the lake in ~ 2200 years (Fig. 4C, orange). Another model, derived using the IPCC A2 scenario, predicts historically low lake levels (1133 m) by the end of the century, and an extension of this rate (0.020 myr^{-1}) indicates that the lake will disappear in as little as 3500 years (Sweagudde, 2009).

At maximum rates of lake level fall (0.129 myr^{-1}), the Nile outlet could disappear in as little as 10 years, depriving Uganda of its main source of electricity, and the water that sustains the Nile during the non-flood stage (Figs. 4C and D; Vanderkelen et al., 2018). If lake level fall continued at those rates, every major port in Lake Victoria could be landlocked within a century, and Kenya would lose all access to the lake within 400 years, while Uganda and Tanzania gain huge areas of potentially arable land (Fig. 4D). This sets up a potentially dangerous dynamic between countries (Uganda and Kenya), which in 2009 fought over ownership of Mbingo Island (Fig. 4D), due to the importance of fishing rights in a lake where over 1 million tons of fish are harvested every year (Kolding et al., 2014). Any decrease in precipitation would only further accelerate the rate of decline of modern Lake Victoria to rates similar to the desiccations that occurred twice between 18 and 14 ka (Broecker et al., 1998; Milly, 1999; Stager et al., 2011) and similar to rates modeled for the late Pleistocene for this study (Fig. 4A), suggesting that Lake Victoria could dry up even more quickly than we model here.

5. Conclusions

Lake Victoria is particularly susceptible to changes in evaporation and precipitation, which many previous models have shown to be the primary drivers in this system. Our model of modern Lake Victoria captures this water balance and is then used to predict how Lake Victoria would respond to changes in evaporation, temperature, precipitation, and insolation in both the past and future. Results indicate that Lake Victoria can drain and refill quickly, but the rate is highly dependent on MAP. Regardless of orbital effects on insolation, Lake Victoria will rapidly desiccate when MAP is 25% less than modern, and once the lake is desiccated, refilling is very slow (>10 kyr) or requires MAP levels very close to modern and high enough precipitation to generate runoff to fill more rapidly (centuries). Thus, based on reconstructed paleoprecipitation using paleosol-based proxies it is likely that Lake Victoria was dry for much, if not all, of the period between 94 and 36 ka. This dry phase likely reflects regional climate phenomena. It coincides with cooler and drier conditions in Gulf of Aden (~ 75 –50 ka), low lake levels in Lakes Tanganyika, Bosumtwi, and Malawi (~ 135 –70 ka), and low to intermediate lake levels at Lake Naivasha between 105 and 60 ka and desiccation between 60 and 35 ka. It is likely that mechanism for this prolonged aridity in the Lake Victoria Basin between 94 and 36 ka was partially a result of eccentricity-enhanced precession, which has been attributed to the East African megadrought. This was followed by high-latitude forcing and cooler SSTs between 70 and 35 ka that reduced convergence of the CAB above Lake Victoria. This previous late Pleistocene desiccation likely had a profound impact on the dispersal and evolution of early modern humans, cichlids, and other fauna in the region. In addition, an extension of rates of lake level decline into the future indicates that termination of Nile outflow and potentially catastrophic impacts for human populations around Lake Victoria is possible within decades, and Kenya could lose access to Lake Victoria within centuries. The results indicate that further regional climate modeling is urgently needed to understand how future climate change will affect this climatically sensitive region.

Acknowledgements

Fieldwork at Rusinga Island and Karungu was conducted under research permits NCST/5/002/R/605 issued to EJB, NCST/RCD/12B/01/07 issued to DJP, NCST/RCD/12B/012/31 issued to JTF, NCST/RCD/12B/012/2 issued to NB, and NCST/5/002/R/576 issued to CAT. We greatly appreciate the support of the National Museum of Kenya (NMK). This work was funded by the National Geographic Society Committee for Research and Exploration (9284-13 and 8762-10), the National Science Foundation (BCS-1013199 and BCS-1013108), the Leakey Foundation, the Geological Society of America, the Society for Sedimentary Geology (SEPM), the University of Queensland, Baylor University, the Baylor University Department of Geosciences Dixon Fund, New York University, Harvard University, and the American School for Prehistoric Research.

Appendix A. Supplementary material

Supplementary material related to this article can be found online at <https://doi.org/10.1016/j.epsl.2019.115883>.

References

- Bard, E., Rostek, F., Sonzogni, C., 1997. Interhemispheric synchrony of the last deglaciation inferred from alkenone palaeothermometry. *Nature* 385, 707–710. <https://doi.org/10.1038/385707a0>.
- Berke, M.A., Johnson, T.C., Werne, J.P., Grice, K., Schouten, S., Sinninghe Damsté, J.S., 2012. Molecular records of climate variability and vegetation response since the Late Pleistocene in the Lake Victoria basin, East Africa. *Quat. Sci. Rev.* 55, 59–74. <https://doi.org/10.1016/j.quascirev.2012.08.014>.
- Beverly, E.J., Driese, S.G., Peppe, D.J., Arellano, L.N., Blegen, N., Tyler Faith, J., Tryon, C.A., Faith, J.T., Tryon, C.A., 2015. Reconstruction of a semi-arid Late Pleistocene paleocatena from the Lake Victoria region, Kenya. *Quat. Res.* 84, 368–381. <https://doi.org/10.1016/j.yqres.2015.08.002>.
- Beverly, E.J., Peppe, D.J., Driese, S.G., Blegen, N., Faith, J.T., Tryon, C.A., Stinchcomb, G.E., 2017. Reconstruction of Late Pleistocene paleoenvironments using bulk geochemistry of paleosols from the Lake Victoria region. *Front. Earth Sci.* 5, 1–12. <https://doi.org/10.3389/feart.2017.00093>.
- Bonnefille, R., Chalief, F., 2000. Pollen-inferred precipitation time-series from equatorial mountains, Africa, the last 40 kyr B.P. *Glob. Planet. Change* 26, 25–50.
- Boven, A., Pasteels, P., Punzalan, L.E., Yamba, T.K., Musisi, J.H., 1998. Quaternary perpotassic magmatism in Uganda (Toro-Ankole volcanic province): age assessment and significance for magmatic evolution along the East African Rift. *J. Afr. Earth Sci.* 26, 463–476. [https://doi.org/10.1016/S0899-5362\(98\)00026-8](https://doi.org/10.1016/S0899-5362(98)00026-8).
- Broecker, W.S., Peteet, D., Hajdas, I., Lin, J., Clark, E., 1998. Antiphasing between rainfall in Africa's Rift Valley and North America's Great Basin. *Quat. Res.* 50, 12–20.
- Budyko, M.I., 1974. *Climate and Life*. Academic Press, New York.
- Claussen, M., Kubatzki, C., Brovkin, V., Ganopolski, A., Hoelzmann, P., Pachur, H.-J., 1999. Simulation of an abrupt change in Saharan vegetation in the mid-Holocene. *Geophys. Res. Lett.* 26, 2037–2040.
- Clement, A.C., Hall, A., Broccoli, A.J., 2004. The importance of precessional signals in the tropical climate. *Clim. Dyn.* 22, 327–341. <https://doi.org/10.1007/s00382-003-0375-8>.
- Cogley, J.G., 1979. The albedo of water as a function of latitude. *Mon. Weather Rev.* 107, 775–781.
- Costa, K., Russell, J., Konecky, B., Lamb, H., 2014. Isotopic reconstruction of the African Humid Period and Congo Air Boundary migration at Lake Tana, Ethiopia. *Quat. Sci. Rev.* 83, 58–67. <https://doi.org/10.1016/j.quascirev.2013.10.031>.
- Danley, P.D., Husemann, M., Ding, B., Dipietro, L.M., Beverly, E.J., Peppe, D.J., 2012. The impact of the geologic history and paleoclimate on the diversification of East African cichlids. *Int. J. Evol. Biol.* 2012, 574851. <https://doi.org/10.1155/2012/574851>.
- Doornkamp, J.C., Temple, P.H., 1966. Surface, drainage and tectonic instability in part of southern Uganda. *Geogr. J.* 132, 238–252.
- East African Meteorological Department, 1972. *Climatological Statistics for East Africa*, vols. 1–3. E.A. Community, Nairobi, Kenya.
- Glassy, J.M., Running, S.W., 1994. Validating diurnal climatology logic of the MT-CLIM model across a climatic gradient in Oregon. *Ecol. Appl.* 4, 248–257. <https://doi.org/10.2307/1941931>.
- Howell, P., Lock, M., Cobb, S. (Eds.), 1988. *The Jonglei Canal: Impact and Opportunity*. Cambridge University Press, New York.
- Ivory, S.J., Blome, M.W., King, J.W., McGlue, M.M., Cole, J.E., Cohen, A.S., 2016. Environmental change explains cichlid adaptive radiation at Lake Malawi over the past 1.2 million years. *Proc. Natl. Acad. Sci.* 113, 11895–11900. <https://doi.org/10.1073/pnas.1611028113>.

- Johnson, T.C., Scholz, C.A., Talbot, M.R., Kelts, K., Ricketts, R.D., Ngobi, G., Beuning, K.R., Ssemmanda, I., McGill, J.W., 1996. Late Pleistocene dessiccation of Lake Victoria and rapid evolution of cichlid fishes. *Science* 273, 1091–1093.
- Johnson, T.C., Werne, J.P., Brown, E.T., Abbott, A., Berke, M., Steinman, B.A., Halbur, J., Contreras, S., Grosshuesch, S., Deino, A., Scholz, C.A., Lyons, R.P., Schouten, S., Damsté, J.S.S., 2016. A progressively wetter climate in southern East Africa over the past 1.3 million years. *Nature* 537, 220–224. <https://doi.org/10.1038/nature19065>.
- Kolding, J., Medard, M., Mkumbo, O., van Sweiten, P., 2014. Status, trends and management of the Lake Victoria fisheries. In: Welcomme, R., Valbo-Jorgensen Halls, J.A. (Eds.), *Inland Fisheries Evolution: Case Studies from Four Continents. Food and Agriculture Organisation of the United Nations, Rome*, pp. 49–62.
- Laskar, J., Robutel, P., Joutel, F., Gastineau, M., Correia, A.C.M., Levrard, B., 2004. A long-term numerical solution for the insolation quantities of the Earth. *Astron. Astrophys.* 428, 261–285. <https://doi.org/10.1051/0004-6361:20041335>.
- Lyon, B., Vigaud, N., 2017. Unraveling East Africa's climate paradox. In: Simon Wang, S.-Y., Yoon, J.-H., Funk, C.C., Gillies, R.R. (Eds.), *Climate Extremes: Patterns and Mechanisms*. In: *Geophysical Monograph*, vol. 226. John Wiley & Sons, Inc., pp. 265–281.
- Lyons, R.P., Kroll, C.N., Scholz, C.A., 2011. An energy-balance hydrologic model for the Lake Malawi Rift Basin, East Africa. *Glob. Planet. Change* 75, 83–97. <https://doi.org/10.1016/j.gloplacha.2010.10.010>.
- McJannet, D.L., Webster, I.T., Cook, F.J., 2012. An area-dependent wind function for estimating open water evaporation using land-based meteorological data. *Environ. Model. Softw.* 31, 76–83. <https://doi.org/10.1016/j.envsoft.2011.11.017>.
- Milly, P.C.D., 1999. Comment on "Antiphasing between rainfall in Africa's Rift Valley and North America's Great Basin". *Quat. Res.* 51, 104–107.
- Moernaut, J., Verschuren, D., Charlet, F., Kristen, I., Fagot, M., De Batist, M., 2010. The seismic-stratigraphic record of lake-level fluctuations in Lake Challa: hydrological stability and change in equatorial East Africa over the last 140 kyr. *Earth Planet. Sci. Lett.* 290, 214–223. <https://doi.org/10.1016/j.epsl.2009.12.023>.
- Monteith, J., Unsworth, M., 2008. *Principles of Environmental Physics*, 3rd edition. Academic Press, Amsterdam.
- Niang, I., Ruppel, O.C., Abdrabo, M.A., Essel, A., Lennard, C., Padgham, J., Urquhart, P., 2014. Africa. In: Barros, V.R., Field, C.B., Dokken, D.J., Mastrandrea, M.D., Mach, K.J., Biliir, T.E., Chatterjee, M., Ebi, K.L., Estrada, Y.O., Genova, R.C., Girma, B., Kissel, E.S., Levy, A.N., MacCracken, S., Mastrandrea, P.R., White, L.L. (Eds.), *Climate Change 2014: Impacts, Adaptation, and Vulnerability. Part B: Regional Aspects. Contribution of Working Group II to the Fifth Assessment Report of the Intergovernmental Panel on Climate Change*. Cambridge University Press, New York, pp. 1199–1265.
- Nicholson, S.E., 1996. A review of climate dynamics and climate variability in Eastern Africa. In: Johnson, T.C., Odada, E.O. (Eds.), *The Limnology, Climatology and Paleoclimatology of the East African Lakes*. Gordon and Breach Publishers, Netherlands, pp. 25–56.
- Nicholson, S.E., 2018. The ITCZ and the seasonal cycle over equatorial Africa. *Bull. Am. Meteorol. Soc.* 99, 337–348. <https://doi.org/10.1175/BAMS-D-16-0287.1>.
- Nordt, L.C., Driese, S.G., 2010. New weathering index improves paleorainfall estimates from Vertisols. *Geology* 38, 407–410. <https://doi.org/10.1130/g30689.1>.
- Rial, J.A., Sr, R.A.P., Beniston, M., Noblet-ducoudré, N.D.E., Prinn, R., 2004. Nonlinearities, feedbacks and critical thresholds within the Earth's climate system. *Clim. Change* 65, 11–38.
- Rowell, D.P., Booth, B.B.B., Nicholson, S.E., Good, P., 2015. Reconciling past and future rainfall trends over East Africa. *J. Climate* 28, 9768–9788. <https://doi.org/10.1175/JCLI-D-15-0140.1>.
- Scholz, C.A., Johnson, T.C., Cohen, A.S., King, J.W., Peck, J.A., Overpeck, J.T., Talbot, M.R., Brown, E.T., Kalindekafu, L., Amoko, P.Y.O., Lyons, R.P., Shanahan, T.M., Castañeda, I.S., Heil, C.W., Forman, S.L., McHargue, L.R., Beuning, K.R., Gomez, J., Pierson, J., 2007. East African megadroughts between 135 and 75 thousand years ago and bearing on early-modern human origins. *Proc. Natl. Acad. Sci. USA* 104, 16416–16421. <https://doi.org/10.1073/pnas.0703874104>.
- Shahin, M., 1985. *Hydrology of the Nile Basin*. Elsevier, Amsterdam.
- Sheldon, N.D., Retallack, G.J., Tanaka, S., 2002. Geochemical climofunctions from North America soils and applications to paleosols across the Eocene-Oligocene boundary in Oregon. *J. Geol.* 110, 687–696.
- Stager, J.C., Johnson, T.C., 2008. The late Pleistocene desiccation of Lake Victoria and the origin of its endemic biota. *Hydrobiologia* 596, 5–16. <https://doi.org/10.1007/s10750-007-9158-2>.
- Stager, J.C., Ryves, D.B., Chase, B.M., Pausata, F.S.R., 2011. Catastrophic drought in the Afro-Asian monsoon region during Heinrich event 1. *Science* 331, 1299–1302. <https://doi.org/10.1126/science.1198322>.
- Stinchcomb, G.E., Nordt, L.C., Driese, S.G., Lukens, W.E., Williamson, F.C., Tubbs, J.D., 2016. A data-driven spline model designed to predict paleoclimate using paleo-ol geochemistry. *Am. J. Sci.* <https://doi.org/10.2475/08.2016.02>.
- Sutcliffe, J.V., Parks, Y.P., 1999. The hydrology of the Nile. *IAHS Spec. Publ.* 5, 192.
- Sutcliffe, J.V., Petersen, G., 2007. Lake Victoria: derivation of a corrected natural water level series. *Hydrol. Sci. J.* 52, 1316–1321. <https://doi.org/10.1623/hysj.52.6.1316>.
- Sweagudde, S.M., 2009. Lake Victoria's water budget and the potential effects of climate change in the 21st century. *Afr. J. Trop. Hydrobiol. Fish.* 30, 22–30.
- Talbot, M.R., Williams, M.A.J., 2009. Cenozoic evolution of the Nile Basin. In: Dumont, H.J. (Ed.), *The Nile: Origin, Environments, Limnology and Human Use*. Springer Science + Business Media B.V., pp. 37–60.
- Thiery, W., Panitz, H.-J., Davin, E., Van Lipzig, N., 2015. The impact of the African Great Lakes on the regional climate. *J. Climate* 28. <https://doi.org/10.1175/JCLI-D-14-00565.1>. 4061+.
- Tierney, J.E., deMenocal, P.B., Zander, P.D., 2017. A climatic context for the out-of-Africa migration. *Geology*, 1–4. <https://doi.org/10.1130/G39457.1>.
- Tierney, J.E., Russell, J.M., Huang, Y., Damsté, J.S.S., Hopmans, E.C., Cohen, A.S., 2008. Northern hemisphere controls on tropical southeast African climate during the past 60,000 years. *Science* 322, 252–255. <https://doi.org/10.1126/science.1160485>.
- Trauth, M.H., Deino, A.L., Bergner, A.G.N., Strecker, M.R., 2003. East African climate change and orbital forcing during the last 175 kyr BP. *Earth Planet. Sci. Lett.* 206, 297–313. [https://doi.org/10.1016/S0012-821X\(02\)01105-6](https://doi.org/10.1016/S0012-821X(02)01105-6).
- Tryon, C.A., Faith, J.T., Peppe, D.J., Beverly, E.J., Blegen, N., Blumenthal, S.A., Chritz, K.L., Driese, S.G., Patterson, D., Sharp, W.D., 2016. The Pleistocene prehistory of the Lake Victoria basin. *Quat. Int.* 404 (Part B), 100–114. <https://doi.org/10.1016/j.quaint.2015.11.073>.
- Vanderkelen, I., van Lipzig, N.P.M., Thiery, W., 2018. Modelling the water balance of Lake Victoria (East Africa) – Part 1: observational analysis. *Hydrol. Earth Syst. Sci.* 22, 5509–5525. <https://doi.org/10.5194/hess-22-5509-2018>.
- Verschuren, D., Johnson, T.C., Kling, H.J., Edgington, D.N., Leavitt, P.R., Brown, E.T., Talbot, M.R., Hecky, R.E., 2002. History and timing of human impact on Lake Victoria, East Africa. *Proc. R. Soc. Lond. B* 269, 289–294. <https://doi.org/10.1098/rspb.2001.1850>.
- Verschuren, D., Sinninghe Damsté, J.S., Moernaut, J., Kristen, I., Blaauw, M., Fagot, M., Haug, G.H., 2009. Half-precessional dynamics of monsoon rainfall near the East African equator. *Nature* 462, 637–641. <https://doi.org/10.1038/nature08520>.
- Wang, Y., Cheng, H., Edwards, R.L., Kong, X., Shao, X., Chen, S., Wu, J., Jiang, X., Wang, X., An, Z., 2008. Millennial- and orbital-scale changes in the East Asian monsoon over the past 224,000 years. *Nature* 451, 1090–1093. <https://doi.org/10.1038/nature06692>.
- Weldeab, S., Lea, D.W., Schneider, R.R., Andersen, N., 2007. 155,000 years of West African monsoon and ocean thermal evolution. *Science* 316, 1303–1307. <https://doi.org/10.1126/science.1140461>.
- Wigley, T.M.L., Jones, P.D., 1985. Influences of precipitation changes and direct CO₂ effects on streamflow. *Nature* 314, 149–152. <https://doi.org/10.1038/314149a0>.
- Yin, X., Nicholson, S.E., 1998. The water balance of Lake Victoria. *Hydrol. Sci. J.*